JMEPEG (2014) 23:2265–2273
DOI: 10.1007/s11665-014-0971-2

1059-9495/$19.00

Effects of pH Value on Corrosion Behavior of Thermal-Sprayed Al-Si Coated Q235 Steel in Simulated Soil Solutions

Xinqiang Wu, Jian Xu, Wei Ke, Song Xu, Bing Feng, and Botao Hu

(Submitted December 26, 2013; in revised form February 13, 2014; published online April 8, 2014)

Electrochemical corrosion behavior of a thermal-sprayed Al-Si coated Q235 steel has been investigated in simulated soil solutions. The as-received Q235 steel and galvanized steel for grounding grids were also examined for comparison purpose. The effects of pH value of testing solutions have been examined. The thermal-sprayed Al-Si coated steel showed better corrosion resistance in acidic and neutral solutions than the as-received Q235 steel and galvanized steel, having the largest polarization resistance, the lowest anodic current density, and the largest film resistance. However, in strong alkaline solution, the corrosion resistance of the thermal-sprayed Al-Si coated steel degraded rapidly due to the change of corrosion product scale. Related corrosion mechanisms are also discussed.

Keywords corrosion scale, electrochemical corrosion, grounding grids, pH value, soil solutions, thermal-sprayed coated steel

1. Introduction

The grounding grids play an important role in stabilizing operation of power system and safeguarding operators and power equipments, because high lightning or short-circuit currents are usually discharged into earth through them. With increasing capability of transformer substations, more strict requirements are demanded for the safe service of the grounding grids. Although copper materials or stainless steels or copper coated steels have been used as common grounding materials in US, Japan and many European countries (Ref 1-7), ordinary carbon steels typical such as Q235 steel or galvanized steel (hot-dipped Zn coated carbon steel) are being used as one of the main materials for the grounding grids in China due to the shortage of resources, the consideration of economy, and possible corrosion problems of dissimilar metal couple between underground ferrous structures and massive copper grounding grids (Ref 8-11). However, much field experience has showed that the carbon steel or galvanized steel grounding grids suffer from severe corrosion during long-term service in soil, in particular in acidic environments (Ref 12-14). The grounding grids become brittle, ensuing surface detaching and loosening, and even fracture failure. Very serious corrosion failures have been observed for the carbon steel grounding grids after only several year services in many Chinese transformer substations. For long-term service grounding grids, due to electrochemical corrosion of carbon steels in corrosive soil environments and corrosion failures induced by current discharging or stray currents, the cross-section of grounding conductors reduces, even causing them to break, in turn leading to increased grounding resistance and decreased heat stability and current discharging ability of the grounding conductors. As a result, the grounding grids may be burned by fault current, resulting in a high voltage difference in substations, and damaging other main power equipments such as transformer and generator, as well as endangering operators' lives. In addition, it is rather difficult and costly to on-site protect, overhaul, repair, or replace in-service undergrounding grids (Ref 15). It is, thus, necessary to understand the electrochemical corrosion behavior and mechanism of the grounding grids and to develop corresponding protective methods or on-line diagnosis techniques. In the present work, electrochemical corrosion behaviors of Q235 steel, galvanized steel, and thermal-sprayed Al-Si coated Q235 steel have been investigated in simulated soil solutions. Effects of pH value of solutions have been examined. Related corrosion mechanisms are also discussed.

Xinqiang Wu, Jian Xu, and **Wei Ke**, Key Laboratory of Nuclear Materials and Safety Assessment, Liaoning Key Laboratory for Safety and Assessment Technique of Nuclear Materials, Institute of Metal Research, Chinese Academy of Sciences, Shenyang 110016, P. R. China; and **Song Xu, Bing Feng, Botao Hu**, Hunan Electric Power Corporation Research Institute, Changsha 410007, P. R. China. Contact e-mail: xqwu@imr.ac.cn.

2. Experimental

2.1 Experimental Material

The as-received Q235 steel sheet and galvanized steel (hot-dipped Zn coated Q235 steel) sheet for grounding grids from Hunan Provincial Electric Power Corporation, and a kind of thermal-sprayed Al-Si coated Q235 steel sheet were used in the present work. The chemical compositions (wt.%) of the Q235 steel are 0.18C, 0.50Mn, ≤ 0.30Si, ≤ 0.050S, ≤ 0.045P, and Fe balance. The thickness of Zn coating for the galvanized steel is about 85 μm. The Al-Si coating consisting of 94 wt.% Al

and 6 wt.% Si was prepared on the as-received Q235 steel sheet using an arc thermal spraying method. The arc spraying voltage and current are 26 to 28 V and 120 to 130 A, respectively. The arc spraying temperature was about 5000 °C, and the velocity of particle was about 260 m/s. All the specimens investigated in the present work were machined from the as-sprayed Al-Si coating without any other treatment. The thickness of Al-Si coating was about 650 μm. Figure 1 shows the cross-section of thermal-sprayed Al-Si coated Q235 steel and the energy dispersive spectra line scan result.

2.2 Electrochemical Tests

To prepare working electrodes for the electrochemical tests, the specimens were sealed with epoxy resin to expose an area of 1 cm^2. The exposed faces were polished with silicon carbide papers of 800 grit size and rinsed with de-ionized water just before the immersion. A three electrode cell featuring a Pt counter electrode and a saturated calomel reference electrode (SCE) was employed. All the potentials in the paper were given versus this reference electrode. Table 1 shows the simulated soil solutions used in the present work, which are based on the primary anions in soil in Yueyang area, China. The electrolytes were prepared from analytical grade $MgCl{\cdot}6H_2O$, Na_2SO_4, and de-ionized water. All the electrochemical tests were carried out at room temperature in the naturally aerated condition. Both linear polarization measurements and polarization curves were conducted using an EG&G 273A Potentiostat. Linear polarization measurements were performed in the potential range from −20 to 20 mV_{ocp}, and the polarization resistance was fitted by Powersuite software. It is well known that the sweep rate can affect the shape and characteristic parameters of polarization curves. If the scan rate is too rapid, the result may not be representative of the system under the test. On the other hand, if it is too slow, the system may change during the measurement (Ref 16). Actually according to ASTM G5 0.166 mV/s, scan rate is recommended; however, it is not mandatory. Large range of sweep rate has been selected in the previous work, varying from 0.166 to 5 mV/s (Ref 17-20). In the present work, a 0.5 mV/s sweep rate was chosen for linear polarization and polarization curve measurements, which is a moderate one in comparison with those reported in the literature. Electrochemical impedance spectra (EIS) measurements were performed with a frequency response analyzer (EG&G 5210) coupled to a potentiostat (EG&G 273A), using a 10 mV (rms) AC perturbation from 100 kHz to 10 mHz. Fitting was performed with ZSimpwin software. For all EIS measurements, AC perturbation was applied before potentiodynamic tests. Because the EIS was conducted at open circuit potential (OCP), so it would not affect the following potentiodynamic measurements too much. The potentiostatic tests were performed only at pH = 4.79 and 12.26 to further distinguish the difference of low pH and high pH values. The samples were immersed in the solutions, until the steady OCP was obtained. The applied polarization potential was 200 mV above the OCP, and the maintaining time was 20 min. All the electrochemical measurements in the present work were repeated at least twice to check the reproducibility. It was found that the reproducibility of each measurement is good.

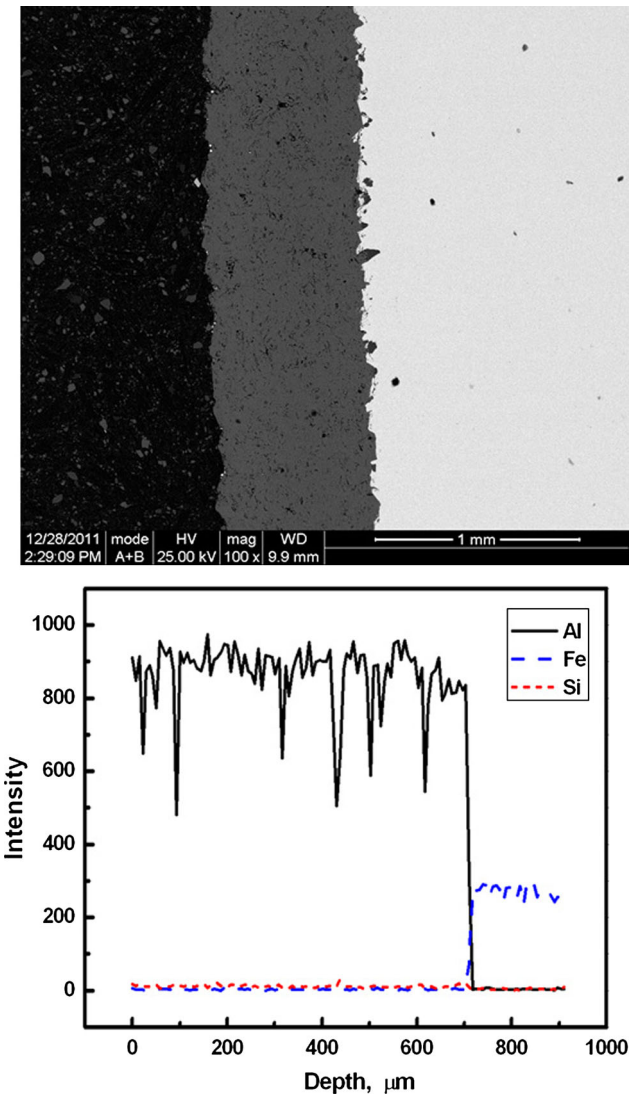

Fig. 1 Cross-section of thermal-sprayed Al-Si coated Q235 steel and energy dispersive spectra line scan result

2.3 Surface Analysis

X-ray photoelectron spectroscopy (XPS) analyses were performed using an ESCALAB 250 x-ray photoelectron spectrometer. Photoelectron emission was excited by monochromatic Al Kα source operated at 150 W with initial photo energy 1486.6 eV. A survey spectrum was first recorded to identify all elements present at the surface, and then high resolution spectra of the following regions were recorded: Al 2p, Si 2p, Fe 2p, and C 1 s. The C 1 s peak from contaminative carbon at 285 eV was used as a reference to correct the

Table 1 Simulated soil solutions used in the present work

Solutions	pH value	Na_2SO_4 (mg/L)	$NaHSO_4{\cdot}H_2O$ (mg/L)	$MgCl_2{\cdot}6H_2O$ (mg/L)	NaOH (mg/L)
1	3.53		447.5	26.04	
2	4.79		8.95	26.04	
3	7.03	9.216		26.04	
4	9.60	9.216		26.04	4
5	12.26	9.216		26.04	400

Table 2 Fitted polarization resistance values (Ω/cm^2)

pH value	Q235 steel	Galvanized steel	Al-Si coating
3.53	619	2890	10,193
4.97	13,681	27,345	33,372
7.03	15,400	55,865	266,200
9.60	9207	36,729	18,312
12.26	403,926	51,117	327

charging shifts. The quantification of the species in the oxide films was performed via XPSpeak 4.1 peak fitting software.

3. Results

Table 2 shows the fitted polarization resistance values at different pH values. It is clear that the polarization resistance of coating materials is dependent on the pH value. In acidic or near neutral solutions, the Al-Si coated Q235 steel showed largest polarization resistance. The galvanized steel had bigger polarization resistance than the Q235 steel. However, in weak alkaline solution, the polarization resistance of Al-Si coated Q235 steel decreased rapidly; the galvanized steel showed the largest polarization resistance. In strong alkaline solution, the Al-Si coated Q235 steel had smallest polarization resistance, while the Q235 steel showed the largest polarization resistance. The above results suggest that the thermal-sprayed Al-Si coated Q235 steel has better corrosion resistance in acidic or near neutral soil environments.

Figure 2 shows the polarization curves at different pH values. All the working electrodes investigated presently showed characteristic of anodic dissolution. No obvious passive region was observed on the polarization curves. In acidic or weak alkaline solutions, the anodic current density of Al-Si coated Q235 steel is relatively low in comparison with that of the as-received Q235 steel and galvanized steel. The lower the pH value, the smaller the anodic current density for the Al-Si coated steel. The corrosion potential of Al-Si coated steel decreased obviously with increasing pH value, while the corrosion potential of the galvanized steel to some extent increased with increasing pH value. In strong alkaline solution, the anodic current density for Al-Si coated steel increased rapidly and is much higher than those for the as-received Q235 steel and galvanized steel, which is in good agreement with the previous linear polarization measurement results.

Figure 3 shows the EIS results at different pH values. Two equivalent circuits based on circuit description code, namely, $R_{sol}(C_{dl}R_{trans})(Q_{film}R_{film})(LR)$ for Q235 steel and galvanized steel and $R_{sol}(C_{dl}R_{trans})(Q_{film}R_{film})$ for Al-Si coated Q235 steel, were used to fit the present EIS data, in which 2 *RC* are in series. Here R_{sol} denotes the resistance of the solution, C_{dl} is the capacitance of the double layer, R_{trans} is the resistance of charge transfer, Q_{film} is the capacitance of the film, and R_{film} is the resistance of the film. An inductance was used in the equivalent circuit, because an apparent inductive loop occurs at low frequency. The appearance of inductive loop is always confusing and it may be related to the iron dissolution characteristics (Ref 21) and possibly related to the presence of chloride ions (Ref 22). But the exact meaning is still unclear. Actually this is a disadvantage of the equivalent circuit analysis, because it is hard to find a physical/chemical process or element corresponding to inductance. The *R* in series with *L* is just used to fit the present EIS data, and its exact meaning is also unclear. However, the main aim of the present work is to investigate pH effects on corrosion behavior of Al-Si coated Q235, and R_{film} is the most important parameter. The equivalent circuits and corresponding fitted parameters are listed in Table 3. In acidic or weak alkaline solutions, the R_{film} for Al-Si coated steel was obviously larger than those for the as-received Q235 steel and galvanized steel, in particular at low pH value. This is obvious on the Bode plots. In strong alkaline solution, the R_{film} for Al-Si coated steel decreased rapidly, agreeing well with the previous polarization measurement results.

Figure 4 shows the results of potentiostatic tests at pH = 4.79 and 12.26 for the above three kinds of materials. Obviously, the Al-Si coated Q235 steel showed much lower current density in acidic solution than the as-received Q235 steel and galvanized steel. However, the current density of the Al-Si coated Q235 steel increased rapidly in strong alkaline solution.

Figure 5 shows the surface morphologies of the above three kinds of materials before and after polarization tests under constant potential. At pH = 4.79, the surface of the as-received Q235 steel appeared russet after polarization test (Fig. 5a and b). The surface of galvanized steel seemed to be corroded to some extent after polarization test (Fig. 5c and d), while the surface of Al-Si coated steel showed no obvious change (Fig. 5e and f). However, after polarization test at pH = 12.26, the surface of Al-Si coated steel certainly suffered from corrosion (Fig. 5g and h).

Figure 6 shows the XPS surface survey spectra recorded from the above three kinds of materials after the potentiostatic tests at pH = 4.79 and 12.26. The corrosion products on both the as-received Q235 steel and galvanized steel mainly consisted of Fe-rich oxides. No Zn signal was detected on the galvanized steel, perhaps due to the dissolution of Zn coating in the testing solution. The detected Mo signal on the galvanized steel may be due to passivation treatment using molybdate salts during hot-dipped Zn coating process. It should be noted that Al, Si, and Fe have been detected on thermal-sprayed Al-Si coated Q235 steel in both solutions with different pH values. However, at pH = 4.79, Al was dominant in the corrosion product, while only a few amount of Si and Fe was detected (Fig. 6c). At pH = 12.26, the amount of Si and Fe in the corrosion product increased obviously (Fig. 6d). Figure 7 shows the Al 2p, Si 2p, and Fe 2p core level spectra recorded from the corrosion product scales on the Al-Si coated Q235 steel in both solutions. At pH = 4.79, AlO(OH) was detected besides Al_2O_3, SiO_2, and Fe_2O_3. At pH = 12.26, no AlO(OH) was detected except for Al_2O_3 and Fe_2O_3, while Si appeared in form of O_2/Si.

Figure 8 shows the surface morphologies of the as-received Q235 steel, galvanized steel, and thermal-sprayed Al-Si coated Q235 steel after one-year bury in an acidic soil in southwest area in China. The Q235 steel has suffered serious corrosion with a russet rust scale formed on the specimen surface (Fig. 8a). Under high magnification, some obvious spallations were observed in the rust scale (Fig. 8b). The galvanized steel showed better corrosion resistance than the as-received Q235 steel. The traces of russet rust were observed in local areas on the specimen surface (Fig. 8c). No obvious spallation took place in the rust scale (Fig. 8d). The thermal-sprayed Al-Si coated Q235 steel had the best corrosion resistance among the

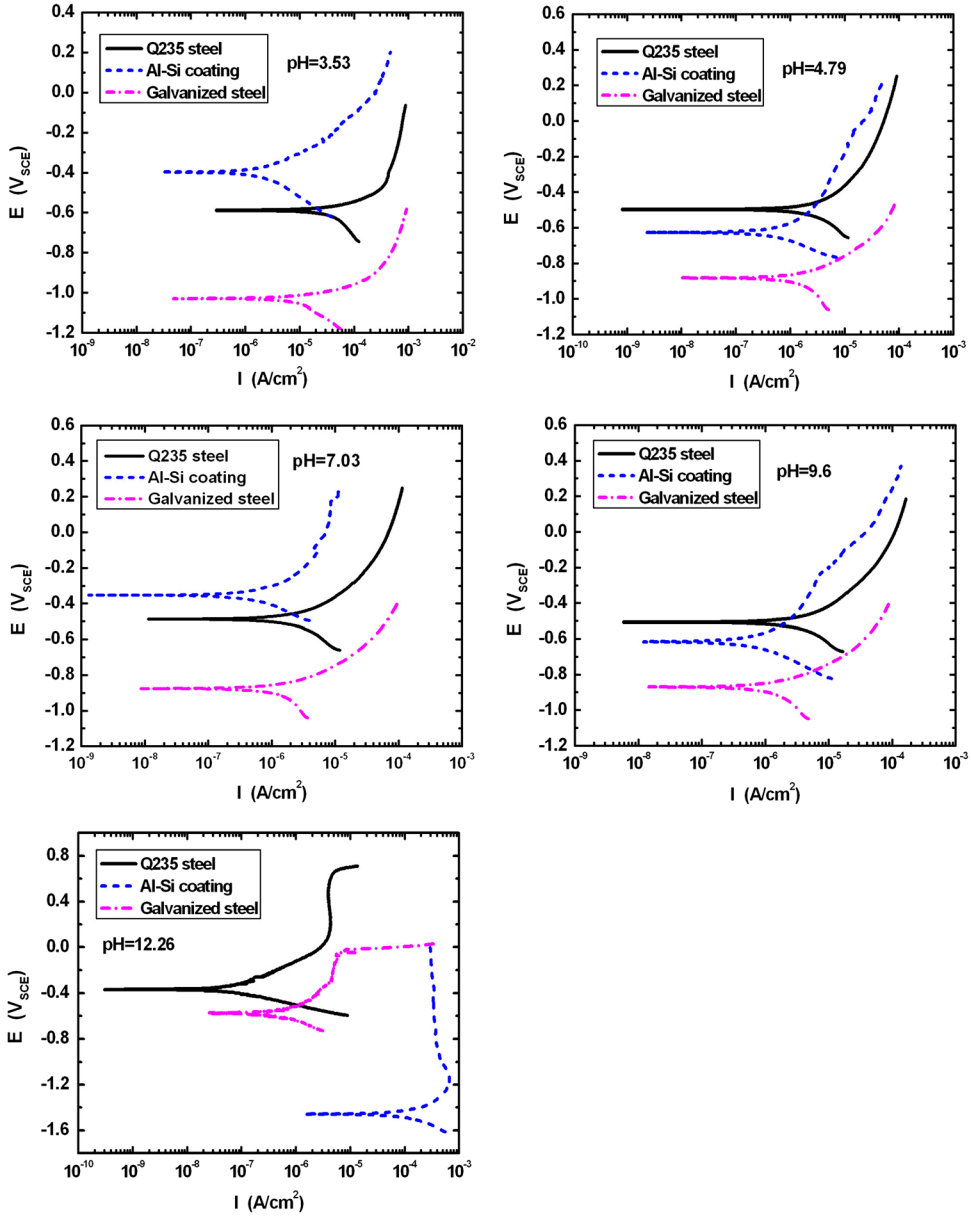

Fig. 2 Polarization curves at different pH values

three kinds of materials. No rust was observed on the specimen surface (Fig. 8e). The original grinding traces clearly remained on the specimen surface under high magnification (Fig. 8f).

4. Discussions

The present electrochemical test results suggest that the thermal-sprayed Al-Si coated Q235 steel has better corrosion resistance in acidic or near neutral soil environments than as-received Q235 steel and galvanized steel (hot-dipped Zn coated Q235 steel). The Al-Si coated steel showed the largest polarization resistance (Fig. 2; Table 2), the lowest anodic current density (Fig. 3), and the largest film resistance (Fig. 4; Table 3) in acidic or neutral soil solutions. However, with increasing pH value, the corrosion resistance of the Al-Si coated steel tended to degrade, in particular in strong alkaline solution. It is believed that the above pH dependent corrosion resistance of the Al-Si coated steel is closely related to the corrosion product scales formed.

The thermodynamic stability of the corrosion products could be evaluated using potential (E)-pH equilibrium diagrams for the systems of M-H_2O (M = Al, Si, Fe, Zn) at 25 °C proposed by Pourbaix (Ref 23). According to the E-pH diagrams of Al-H_2O and Si-H_2O, Al_2O_3 and SiO_2 are the stable corrosion products in acidic or weak alkaline solutions, while Al tends to dissolve in form of AlO_2^-, and Si tends to dissolve in form of SiO_3^{2-} in strong alkaline solutions. The XPS analyses in the present work are in good agreement with the above thermodynamic prediction. At pH = 4.79, Al was dominant in the corrosion product in form of Al_2O_3 and AlO(OH), while only a few amount of Si and Fe was detected in form of SiO_2 and Fe_2O_3 (Fig. 7). At pH = 12.26, no AlO(OH) was detected

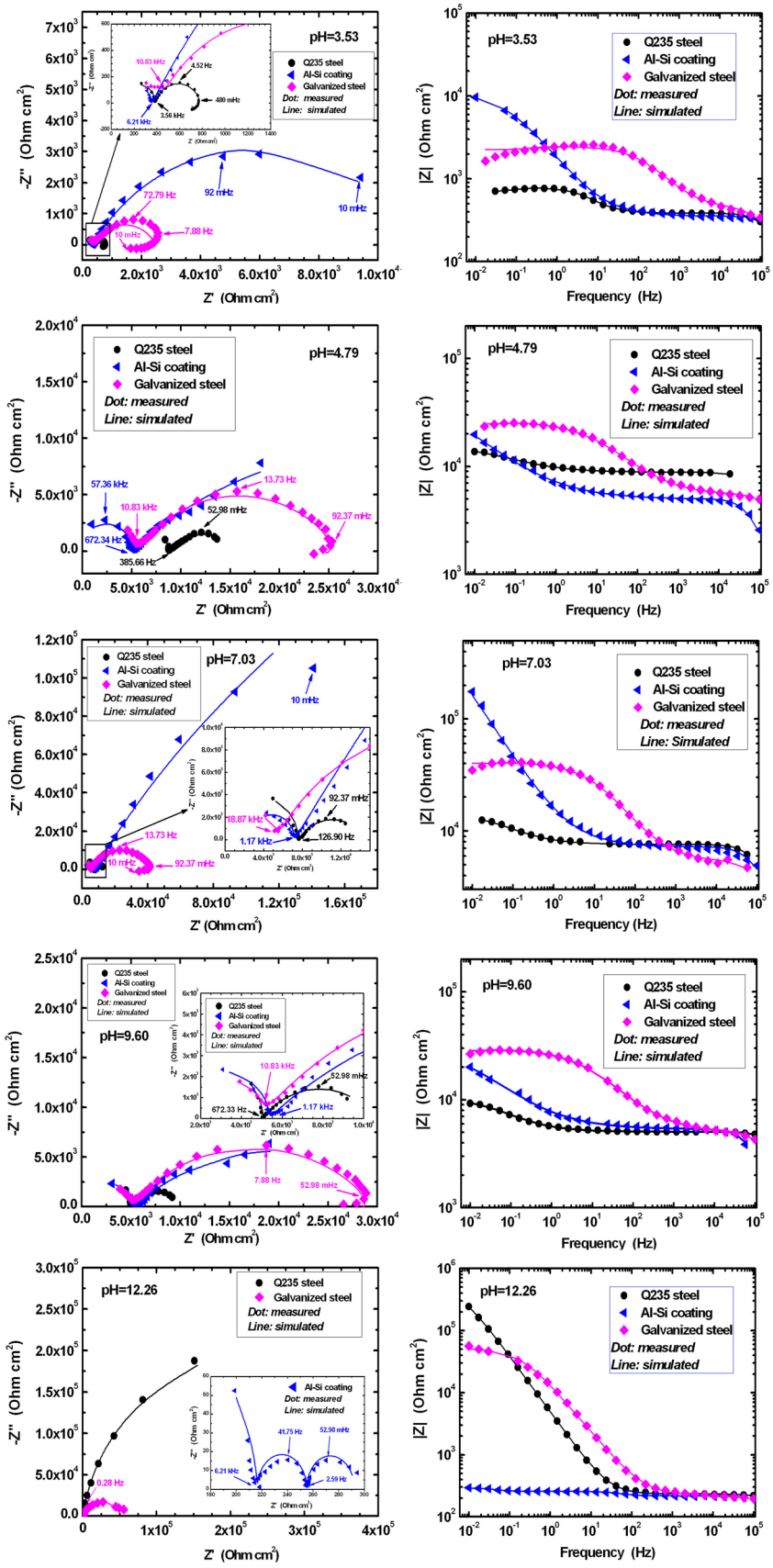

Fig. 3 EIS results at different pH values

Table 3 Equivalent circuit and corresponding fitted parameters

pH	Materials	Equivalent circuit	C_{dl} (F/cm^2)	R_{trans} (Ohm cm^2)	Q_{film} (F/cm^2)	n	R_{film} (Ohm cm^2)	L or C (H cm^2) or (F cm^2)	R (Ohm cm^2)
3.53	Q235 steel	$R_{sol}(C_{dl}R_{trans})(Q_{film}R_{film})$(LR)	4.9×10^{-9}	287.9	1.48×10^{-4}	0.810	4.11×10^{2}	176.3	95.91
	Galvanized steel	$R_{sol}(C_{dl}R_{trans})(Q_{film}R_{film})$(LR)	1.17×10^{-8}	207.2	3.84×10^{-6}	0.713	2.05×10^{2}	129.2	221.5
	Al-Si coating	$R_{sol}(C_{dl}R_{trans})(Q_{film}R_{film})$	3.49×10^{-9}	234	1.74×10^{-4}	0.659	1.09×10^{4}	…	…
4.79	Q235 steel	$R_{sol}(C_{dl}R_{trans})(Q_{film}R_{film})$	1.13×10^{-10}	3046	2.77×10^{-4}	0.499	7.19×10^{3}	…	…
	Galvanized steel	$R_{sol}(C_{dl}R_{trans})(Q_{film}R_{film})$(LR)	2.4×10^{-10}	3914	4.15×10^{-6}	0.56	2.09×10^{4}	5282	1489
	Al-Si coating	$R_{sol}(C_{dl}R_{trans})(Q_{film}R_{film})$	5.79×10^{-10}	4972	1.68×10^{-4}	0.431	5.09×10^{4}	…	…
7.03	Q235 steel	$R_{sol}(C_{dl}R_{trans})(Q_{film}R_{film})$	7.38×10^{-10}	4016	2.74×10^{-4}	0.627	4.02×10^{3}	…	…
	Galvanized steel	$R_{sol}(C_{dl}R_{trans})(Q_{film}R_{film})$(LR)	4.23×10^{-10}	4027	1.65×10^{-6}	0.642	3.60×10^{4}	6000	1183
	Al-Si coating	$R_{sol}(C_{dl}R_{trans})(Q_{film}R_{film})$	5.13×10^{-10}	4579	3.01×10^{-5}	0.607	8.58×10^{5}	…	…
9.60	Q235 steel	$R_{sol}(Q_{dl}R_{trans})(Q_{film}R_{film})$	1.13×10^{-10}	5049	3.57×10^{-4}	0.597	5.55×10^{3}	…	…
	Galvanized steel	$R_{sol}(C_{dl}R_{trans})(Q_{film}R_{film})$(LR)	3.31×10^{-10}	3486	3.89×10^{-6}	0.563	2.5×10^{4}	8593	1433
	Al-Si coating	$R_{sol}(Q_{dl}R_{trans})(Q_{film}R_{film})$	5.49×10^{-10}	4430	1.37×10^{-4}	0.468	2.91×10^{4}	…	…
12.26	Q235 steel	$R_{sol}(C_{dl}R_{trans})(Q_{film}R_{film})$	3.91×10^{-9}	171.3	3.9×10^{-5}	0.901	4.53×10^{5}	…	…
	Galvanized steel	$R_{sol}(C_{dl}R_{trans})(Q_{film}R_{film})$	7.35×10^{-9}	139.6	1.62×10^{-5}	0.793	5.21×10^{4}	…	…
	Al-Si coating	$R_{sol}(C_{dl}R_{trans})(Q_{film}R_{film})$(CR)	8.95×10^{-2}	37.19	6.54×10^{-9}	0.96	1.96×10^{2}	6.96×10^{-5}	38.51

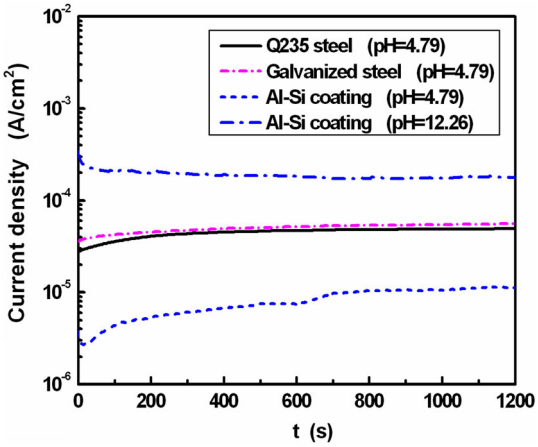

Fig. 4 Potentiostatic tests at pH = 4.79 and 12.26

except for Al_2O_3 and Fe_2O_3, while Si appeared in form of O_2/Si. Moreover, the Al content in the corrosion product scale decreased from 91 to 65 at.% when the pH value increased from 4.79 to 12.26 (Fig. 6), suggesting that more Al in the scale dissolved in the strong alkaline solution. In addition, the change of Si in the scale from SiO_2 at pH = 4.79 to O_2/Si at pH = 12.26 may also degrade protective property of the corrosion product scale. In the present work, the Al-Si coated Q235 steel showed the best corrosion resistance in acidic or weak alkaline solutions among the three kinds of materials. According to XPS analyses and *E*-pH diagrams of Fe-H_2O, Zn-H_2O, Al-H_2O, and Si-H_2O (Ref 16), it is believed that the corrosion product scale consisting of mixture of Al_2O_3, AlO(OH), and SiO_2 on the Al-Si coated Q235 steel is more protective than those consisting of Fe_2O_3 on the as-received Q235 steel or mixture of Fe_2O_3 and Zn-bearing oxide or hydroxide on the galvanized steel.

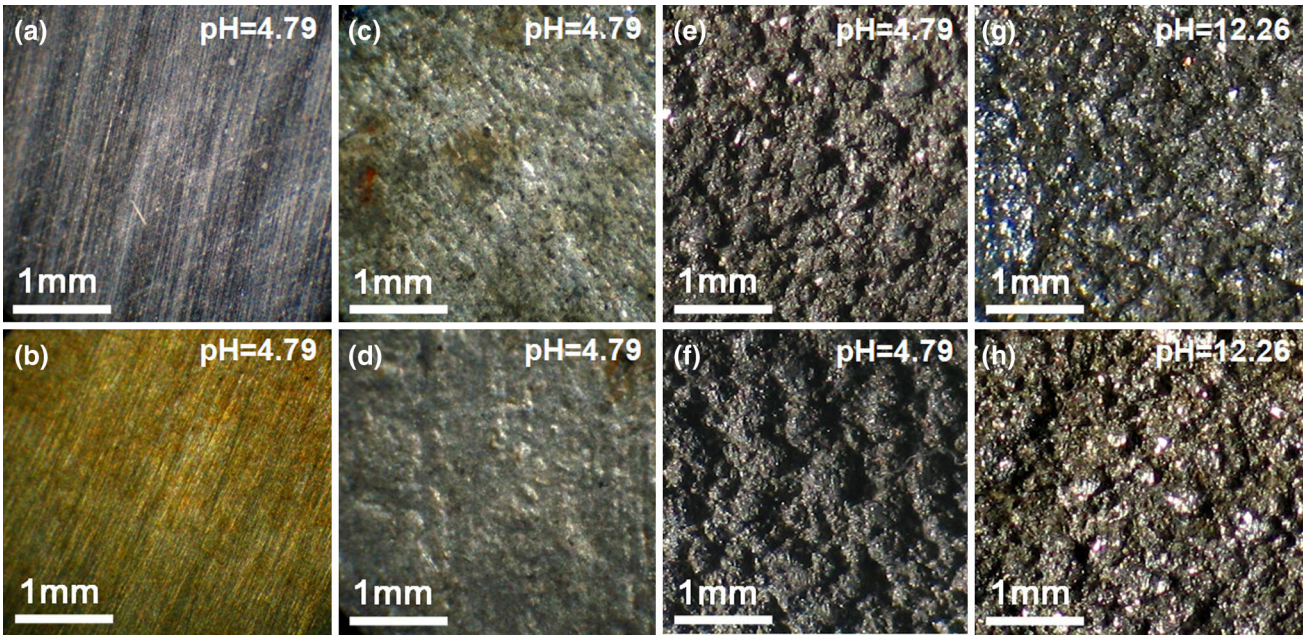

Fig. 5 Surface morphologies (a, c, e, g) before and (b, d, f, h) after potentiostatic tests. (a, b) the as-received Q235 steel, pH = 4.79, (c, d) galvanized steel, pH = 4.79 (e, f) Al-Si coating, pH = 4.79 (g, h) Al-Si coating, pH = 12.26

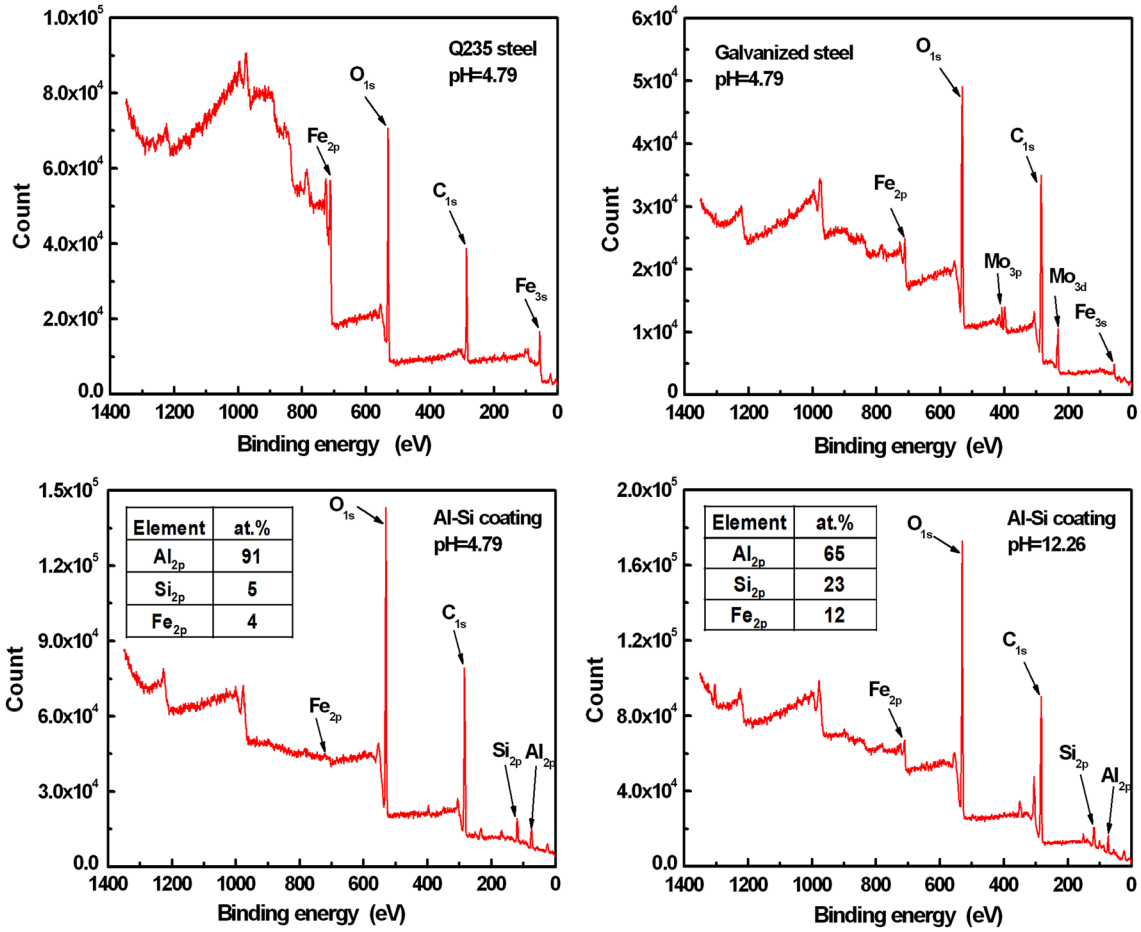

Fig. 6 XPS surface survey spectra recorded from the samples after potentiostatic tests

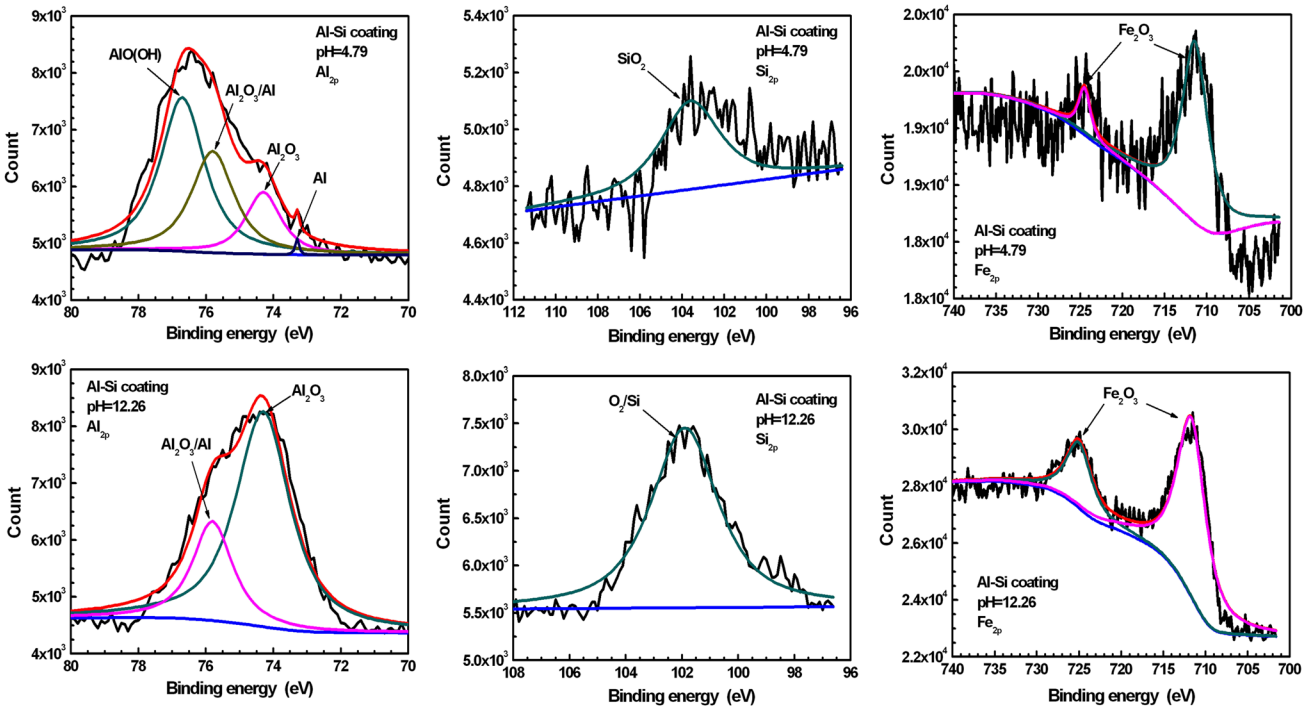

Fig. 7 Al 2p, Si 2p, Fe 2p core level spectra recorded from the corrosion product scales on the Al-Si coated Q235 steel

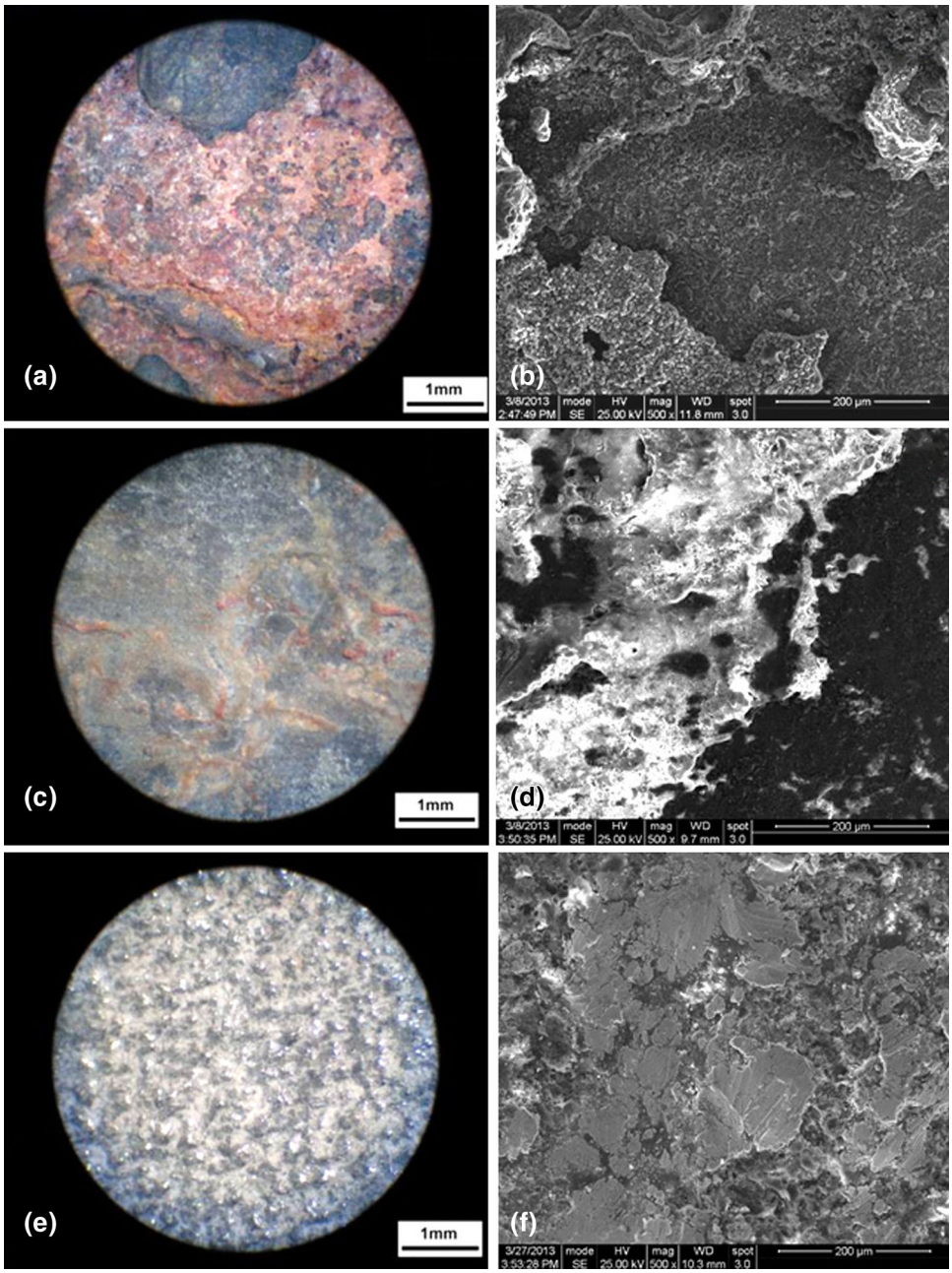

Fig. 8 Surface morphologies of the as-received Q235 steel, galvanized steel, and thermal-sprayed Al-Si coated Q235 steel after one-year bury in an acidic soil in southwest area in China. (a, b) the as-received Q235 steel, (c, d) galvanized steel, (e, f) Al-Si coated Q235 steel

It is very significant to develop economic and effective anti-corrosive metallic materials or coatings for grounding mesh to improve the stability of power system. The present testing results show that the thermal-sprayed Al-Si coated Q235 steel has better anti-corrosion performance in acidic soil solutions than the as-received Q235 steel and galvanized steel, suggesting that such kind of coating may be of great perspective to prolong the service life of grounding mesh. This has been further proved by the one-year field bury tests in an acidic soil in southwest area in China. The thermal-sprayed Al-Si coated Q235 steel had the best corrosion resistance among the above three kinds of materials (Fig. 8).

5. Conclusions

Electrochemical corrosion behaviors of the as-received Q235 steel, galvanized steel, and thermal-sprayed Al-Si coated Q235 steel have been investigated in simulated soil solutions in the present work. Some conclusions could be drawn as follows.

(1) The thermal-sprayed Al-Si coated Q235 steel showed better corrosion resistance in acidic and neutral solutions than the as-received Q235 steel and galvanized steel. However, in strong alkaline solution, its corrosion resistance degraded rapidly.

(2) The pH dependent corrosion resistance of the thermal-sprayed Al-Si coated Q235 steel is due to the corrosion product scales formed. It is believed that the corrosion product scale consisting of mixture of Al_2O_3, AlO(OH), and SiO_2 on the Al-Si coated Q235 steel in acidic solution is more protective than those consisting of Fe_2O_3 on the as-received Q235 steel or mixture of Fe_2O_3 and Zn-bearing oxide on the galvanized steel.

(3) The one-year field bury tests in an acidic soil in southwest area in China prove that the thermal-sprayed Al-Si coated Q235 steel had best corrosion resistance among the above three kinds of materials, suggesting that such kind of coating may be of great perspective to prolong the service life of grounding mesh.

Acknowledgments

This work was jointly supported by the Science Project of State Grid Corporation of China under Grant KG12K16004, the Science and Technology Project of Yunnan Province, the Technology Development (Cooperation) Fund from Yunnan Wenshan Dounan Manganese Industry Co., Ltd. and the Innovation Fund of Institute of Metal Research (IMR), Chinese Academy of Sciences (CAS).

References

1. ANSI/IEEE Standard No. 80-2000, *IEEE Guide for Safety in AC Substation Grounding*, The Institute of Electrical and Electronics Engineers, New York, NY, 2000
2. BS 7430 Standard, *1998 Code of Practice for Earthing*, British Standards Institution, London, 1998
3. ANSI/UL467 Standard, *Grounding and Bonding Equipment*, 9th ed., Canadian Standards Association, Underwriters Laboratories, Canada, 2007
4. M. Loboda and R. Marciniak, Field Corrosion Tests in Poland of Copper Coated Steel Earthing Rods for LPS, *29th International Conference on Lightning Protection*, Uppsala, Sweden, June 2008, p 5–9
5. Y. Li, F.P. Dawalibi, and J. Ma, Grounding System Analysis and Design Considerations for Large Hydroelectric Power Plant, *2012 International Conference on Energy and Environmental Protection (ICEEP 2012)*, Hohhot, Inner Mongolia, China, June 2012, p 6–10
6. P.K. Sen, Steel Grounding, *IEEE Conference Record of Industrial and Commercial Power System Technical Conference*, 1985, p 1–6
7. F.L. Thomas and L.F. Norman, The Effect of Corrosion Mythson National Electrical Standards, *IEEE Trans. Ind. Appl.*, 1993, **29**, p 1006–1011
8. P.P. Zhou, S. Wang, Z.Z. Li, B. Zhang, and R. Zeng, Review of Corrosion Resistant Metals for Grounding, *Electr. Power Constr.*, 2010, **31**, p 50–54
9. Y.Q. Li, C.W. Du, H. Feng, and Y. Zhao, Soil Corrosion of Grounding Electrode, *Environ. Test.*, 2010, **1**, p 15–18
10. M. Romanoff, *Underground Corrosion, NBS Circular 579*, U.S. Department of Commerce, Gaithersburg, MD, 1957
11. P.K. Sen, K. Malmedal, and J.P. Nelson, Steel Grounding Design Guide and Application Notes, *IEEE Rural Electric Power Conference*, Colorado Springs, CO, USA, May 2002, p C2–C2_10
12. C.J. Cai, Investigation on Operation Condition of AC Grounding Network Designed According to Foreign Standard in China, *Electr. Equip.*, 2005, **6**, p 21–25
13. X.W. Hu, C.W. Xu, and Q. Wang, Test of Anti-corrosion Material of Grounding Grid, *High Volt. Eng.*, 2002, **28**, p 21–23
14. V.N. Manohar, Design of Steel Earthing Grids in India, *IEEE Trans. Power Appar. Syst.*, 1979, **PAS 98**, p 11–12
15. V.R. Lawson, Problems and Detection of Line Anchor and Substation Ground Grid Corrosion, *IEEE Transaction on Industry Applications*, 1988, **24**, p 25–32
16. A. Poursaee, Determining the Appropriate Scan Rate to Perform Cyclic Polarization Test on the Steel Bars in Concrete, *Electrochim. Acta*, 2010, **55**, p 1200–1206
17. A. Fattah-alhosseini, A. Saatchi, M.A. Golozar, and K. Raeissi, The Transpassive Dissolution Mechanism of 316L Stainless Steel, *Electrochim. Acta*, 2009, **54**, p 3645–3650
18. Y. Fu, X.Q. Wu, E.H. Han, W. Ke, K. Yang, and Z.H. Jiang, Effects of Cold Work and Sensitization Treatment on the Corrosion Resistance of High Nitrogen Stainless Steel in Chloride Solutions, *Electrochim. Acta*, 2009, **54**, p 1618–1629
19. W. Ye, Y. Li, and F.H. Wang, The Improvement of the Corrosion Resistance of 309 Stainless Steel in the Transpassive Region by Nanocrystallization, *Electrochim. Acta*, 2009, **54**, p 1339–1349
20. B. Deng, Y.M. Jiang, J.L. Xu, T. Sun, J. Gao, L.H. Zhang, W. Zhang, and J. Li, Application of the Modified Electrochemical Potentiodynamic Reactivation Method to Detect Susceptibility to Intergranular Corrosion of a Newly Developed Lean Duplex Stainless Steel LDX2101, *Corros. Sci.*, 2010, **52**, p 969–977
21. M. Keddam, O.R. Mattos, and H. Takenouti, Mechanism of Anodic Dissolution of Iron-chromium Alloys Investigated by Electrode Impedances—I. Experimental Results and Reaction Model, *Electrochim. Acta*, 1986, **31**, p 1147–1158
22. R.F.A. Jargenlius-Pettersson and B.G. Pound, Examination of the Role of Molybdenum in Passivation of Stainless Steels Using AC Impedance Spectroscopy, *J. Electrochem. Soc.*, 1998, **145**, p 1462–1469
23. M. Pourbaix, *Atlas of Electrochemical Equilibria in Aqueous Solutions*, National Association of Corrosion Engineers, Houston, TX, 1974